Title	Fine-tuning to minimize emittances of J-PARC RF-driven H^- ion source
Author(s)	Ueno Akira, Okoshi Kiyonori, Ikegami Kiyoshi, Takagi Akira, Asano Hiroyuki, Oguri Hidetomo
Citation	Review of Scientific Instruments, 87(2), p.02B130_1-02B130_5
Text Version	Publisher's Version
URL	https://jopss.jaea.go.jp/search/servlet/search?5051727
DOI	https://doi.org/10.1063/1.4932573
Right	This article may be downloaded for personal use only. Any other use requires prior permission of the author and the American Institute of Physics. The following article appeared in Review of Scientific Instruments and may be found at https://doi.org/10.1063/1.4932573.

AIP | Review of Scientific Instruments

Fine-tuning to minimize emittances of J-PARC RF-driven H− ion source

A. Ueno, K. Ohkoshi, K. Ikegami, A. Takagi, H. Asano, and H. Oguri

Citation: Review of Scientific Instruments **87**, 02B130 (2016); doi: 10.1063/1.4932573
View online: http://dx.doi.org/10.1063/1.4932573
View Table of Contents: http://scitation.aip.org/content/aip/journal/rsi/87/2?ver=pdfcov
Published by the AIP Publishing

REVIEW OF SCIENTIFIC INSTRUMENTS 87, 02B130 (2016)

Fine-tuning to minimize emittances of J-PARC RF-driven H^- ion source

A. Ueno,[a)] K. Ohkoshi, K. Ikegami, A. Takagi, H. Asano, and H. Oguri
J-PARC Center, Tokai-Mura, Naka-Gun, Ibaraki-Ken 319-1195, Japan

(Presented 25 August 2015; received 21 August 2015; accepted 25 September 2015; published online 4 November 2015)

The Japan Proton Accelerator Research Complex (J-PARC) cesiated RF-driven H^- ion source has been successfully operated for about one year. By the world's brightest level beam, the J-PARC design beam power of 1 MW was successfully demonstrated. In order to minimize the transverse emittances, the rod-filter-field (RFF) was optimized by changing the triple-gap-lengths of each of pairing five piece rod-filter-magnets. The larger emittance degradation seems to be caused by impurity-gases than the RFF. The smaller beam-hole-diameter of the extraction electrode caused the more than expected improvements on not only the emittances but also the peak beam intensity. © *2015 AIP Publishing LLC.* [http://dx.doi.org/10.1063/1.4932573]

I. INTRODUCTION

In the Japan Proton Accelerator Research Complex (J-PARC) second stage starting on October 2014, which is aiming to produce a beam with 1 MW power routinely from the 3 GeV rapid cycling synchrotron (RCS), a newly installed cesiated RF-driven H^- ion source (IS) has been successfully operated without any serious problem for about one year.[1] The J-PARC-IS was developed to satisfy the requirements of a H^- ion beam peak intensity (I_{H^-}) of 60 mA within normalized emittances of 1.5π mm mrad both horizontally and vertically, a flat top beam duty factor of 1.25% (500 μs × 25 Hz) and a lifetime of longer than 1 month[2–4] by using an internal-RF-antenna developed at the Spallation Neutron Source (SNS).[5] As the first priority task of the commissioning to confirm the basic validity of the J-PARC design, the J-PARC design beam power of 1 MW was successfully demonstrated by using an I_{H^-} of 58 mA from the J-PARC-IS for a short period, whose about 88% (50 mA) was accelerated and injected into the RCS. The world's brightest level beam of the J-PARC-IS was realized by several original techniques, such as a 16 mm-thick tapered plasma electrode (PE),[6] a low PE temperature (T_{PE}) operation with precisely controlled cesium (Cs) injection,[2] axial magnetic field correction (AMFC) of the beam extraction region,[7] and so on. The beam loss at each element of the J-PARC is restricted to the threshold value which guarantees the reasonable maintainability of the element. The routine RCS beam power has been gradually increased up to 0.5 MW by the beam tunings during the year. For the 0.5 MW beam power operation, an I_{H^-} of 33 mA, whose transverse emittances are smaller than those for higher intensity beams, is used. Since the beam with smaller emittances is preferable for lower beam-loss operations, the J-PARC-IS is continuously being finely tuned by changing the rod-filter-field (RFF), the beam-hole-diameter of the extraction electrode and so on, on the IS test-stand (IS-TS). The results of the tunings are presented in this paper.

Note: Contributed paper, published as part of the Proceedings of the 16th International Conference on Ion Sources, New York, New York, USA, August 2015.
a)akira.ueno@j-parc.jp.

II. EXPERIMENTAL SETUP AND METHODS

The cross-sectional view of the experimental setup of the IS-TS, which consists of the IS with a stainless steel (SS) plasma chamber (PCH) unitized from an end-flange to a PE, extraction and ground electrodes (EE and GE), an ejection angle correction electromagnet (EACEM), a vacuum chamber for differential pumping by a 1500 l/s turbo-molecular-pump (TMP) with a ceramics insulator duct with an outer diameter of 500 mm and a length of 100 mm for 50 kV insulation, a solenoid magnet (SM), and a vacuum chamber for monitors and a 500 l/s TMP, is shown in Fig. 1.

The IS consists of a SS PCH with eighteen plasma confinement cusp-magnets on the outer-wall and two SS pipes to install rod-filter-magnets (RFMs) cooled by water flowing inside an end-flange with four plasma confinement cusp-magnets on the outer-wall, an internal-RF-antenna, a Cs-injector composed of a Cs-reservoir, a remotely controlled Cs-valve, and a Cs-tube, each of which is temperature controlled by using a thermocouple and a heating mantle attached to it, a PE made of molybdenum, a PE temperature control plate made of oxygen free copper (OFC) attached to the PE and an AMFC coil, whose maximum current (I_{AMFC}) is 13.3 A (1500 AT), located around the downstream flange of the PCH. The I_{H^-} is enhanced more than 10% by the AMFC.[7] The PE temperature (T_{PE}) is controlled by changing the air-flow rate (typically 800 or 1800 l/h) and feed-backing the power of the air temperature control heater, which changes the temperature of the air flowing through a SS pipe brazed on the PE temperature control plate, in order to regulate the control plate temperature (T_{CP}) to the settled value measured by a thermocouple inserted in the pipe and attached to the inner surface of the pipe brazed on the plate. The maximum power of the heater is 500 W. The T_{PE} can be estimated by the equation acquired in the operation of a prototype un-unitized PCH IS as $T_{PE} = 120 + (200 - 120)/(255 - 142) * (T_{CP} - 142)$. The direct measurement of the T_{PE} is difficult in the unitized SS PCH source due to the structural difficulty of the thermocouple installation. The air-flow rate is set to 1800 l/h, which is the maximum value attained by the compressed air with the pressure of 0.7 Mpa, for the T_{PE} lower than 160 °C. It is set to

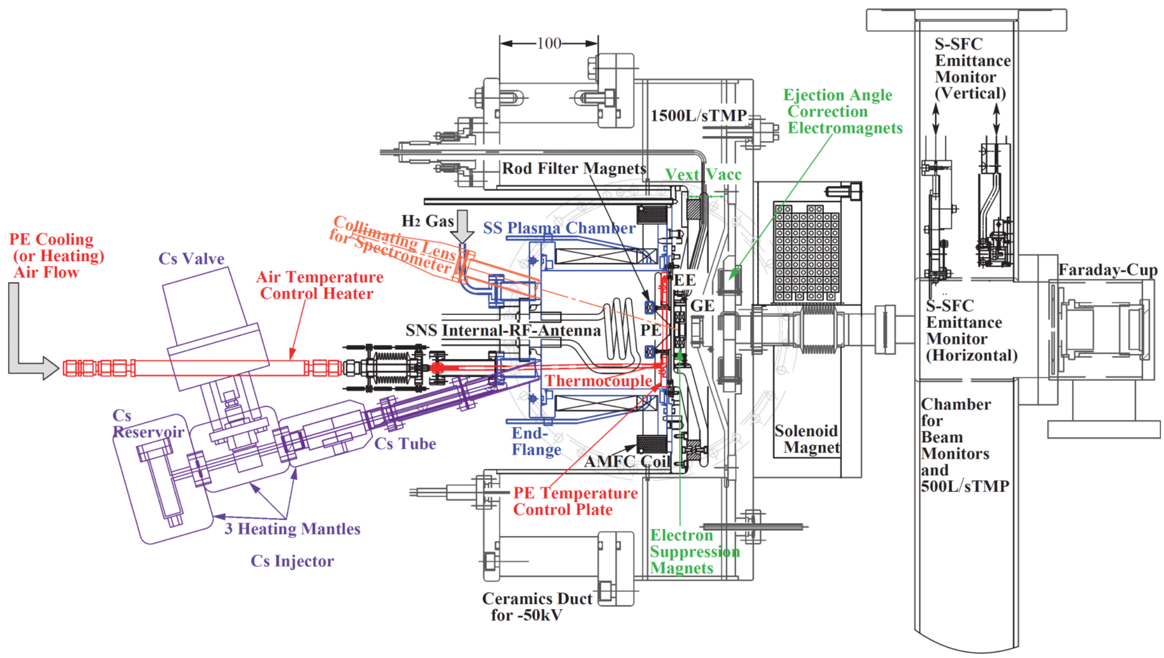

FIG. 1. Cross-sectional view of experimental setup of J-PARC RF-driven H^- ion source test-stand.

typically 800 l/h for the T_{PE} higher than 160 °C. The amount of the Cs in the plasma is monitored by measuring the intensity of 852 nm spectrum with a spectrometer JAZ-EL200-XR,[8] whose collimating lens looking into the beam-hole of the PE is installed on the end-flange.

The H^- ion beam extracted by the extraction voltage (V_{ext}: typically 10 kV) between the PE and the EE is accelerated by the acceleration voltage (V_{acc}: typically 40 kV) between the EE and the GE. The 50 keV H^- beam, which is the design injection energy of the following RFQ (Radio-Frequency Quadrupole linear accelerator), is produced by the 2-gap acceleration. The electrons extracted simultaneously with the H^- ion beam are bent to the electron dump on the EE by the electron suppression permanent magnets made of Ni plated NdFeB permanent magnets installed in the EE. The ejection angle of the H^- ion beam, which is produced by the rod-filter and electron-suppression fields, is corrected with an alignment error of about 50 μm by the EACEM.[6] The ejected H^- ion beam is focused by the SM into the chamber for beam monitors and the 500 l/s TMP. The coil current of the SM was 400 A (56000 AT) for the all operation presented in this paper.

The horizontal and vertical emittances are measured by using two sets of movable slit (S) and movable slit with Faraday-cup (SFC) (S-SFC) emittance monitors. Each slit composed of a pair of tungsten (W) plates has an opening of 0.1 mm. The electric current detected with each SFC is terminated with a 2.5 kΩ terminator, amplified by a factor of 11 and converted to a voltage signal by an operational amplifier. The measured emittance is visualized by randomly plotting dots, whose number is proportional to the voltage signal and is normalized to make the total number of 100 000, in each mesh area defined by the moving steps (typically 0.2 mm and 2 mrad) and the positions of the S and the SFC. The offset of the signal detected with the SFC is compensated by subtracting the baseline value, which is calculated by averaging 40 data of the waveform during 40 μs without 2 MHz-RF plasma, from the signal value, which is calculated by averaging 500 data during 500 μs with 2 MHz-RF plasma. There is a noise reduction effect with the possibility of a slight underestimation of emittance in the conversion from the signal voltage to the finite dots with the number of 100 000. The details of the emittance measurements including the structure of the monitors are presented in Ref. 3.

III. RFF OPTIMIZATION

The measured relationships between the I_{H^-} and the horizontal and vertical rms normalized emittances (ε_{xrmsn} and ε_{yrmsn}) with four PCHs (#2–#5), which were machined with the same design, are shown in Fig. 2. As shown in Fig. 2, the ε_{xrmsn} and ε_{yrmsn} for each condition has almost the same value. Since the ε_{xrmsn} and ε_{yrmsn} of #3 are rather larger than those of #2, #4, or #5, the RFF of #3 was finely tuned by changing the triple-gap-lengths (Gs) of each of the pairing five piece RFMs as shown in Fig. 3. The measured relationships between the I_{H^-} and the ε_{xrmsn} and ε_{yrmsn} for the RFM gap-lengths (Gs) of

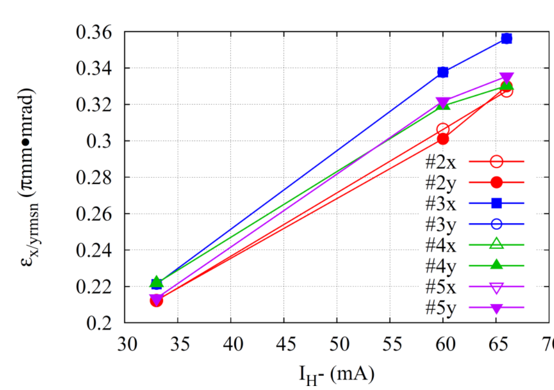

FIG. 2. Measured relationships between I_{H^-} and ε_{xrsmn} and ε_{yrsmn} with four PCHs (#2–#4).

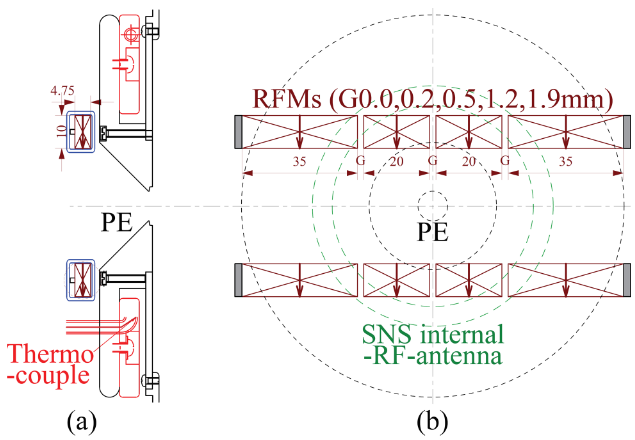

FIG. 3. Drawing of RFMs related with PE and SNS internal-RF-antenna shown by cross-sectional views on beam axis (a) and RFM center of beam axis direction (b).

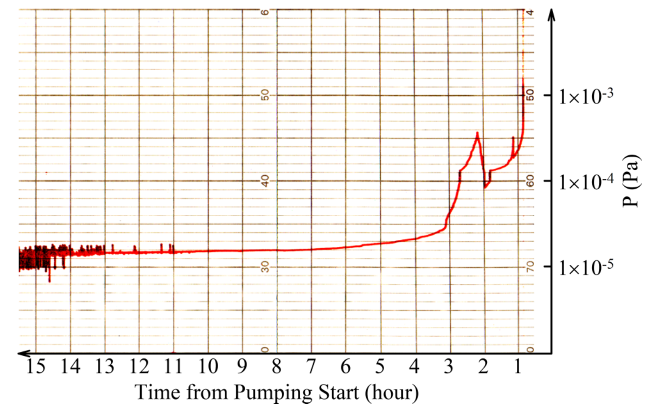

FIG. 5. Observed vacuum pressure fluctuation with #3PCH shown as relationship between time after TMPs start and vacuum pressure (P).

0.0, 0.2, 0.5, 1.2, and 1.9 mm with #3 PCH are shown in Fig. 4. Although the ε_{xrmsn} and ε_{yrmsn} were minimized with G0.5, they were still slightly higher than those with other PCH as shown in Fig. 3. Furthermore, the ε_{xrmsn} and ε_{yrmsn} for every G with #3 PCH degraded up to around 0.36π mm mrad by the following several hour operation. The accumulation of impurity gas is thought to cause the degradation, since the spike-noise-like fluctuations of the vacuum pressure, which started 11 h after the TMPs starts and lasted more than 24 h, were observed as shown in Fig. 5 was observed occasionally only with the #3 PCH. Since the fluctuated elements were identified as argon and nitrogen gases by a quadrupole mass spectrometer, there should be air-pockets in the vacuum region of #3 PCH. The grooves for the O-rings, which are suspected to produce the air-pockets, are under machining to remove them.

IV. BEAM-HOLE-DIAMETER OPTIMIZATION

The effects of the EE beam-hole-diameters (Φ_{EE} = 8.3, 7.7, and 7.1 mm) shown in Fig. 6 on the ε_{xrmsn} and ε_{yrmsn} were investigated. The relationships between the I_{H^-} and the ε_{xrmsn} and ε_{yrmsn} measured for the #4 PCH with the RFMs gap lengths of 1.9 mm (G1.9) are shown in Fig. 7. The ε_{xrmsn} and ε_{yrmsn} for Φ_{EE} of 8.3, 7.7, and 7.1 mm are plotted with open and closed squares, triangles and circles, respectively. The smaller Φ_{EE} produced not only the smaller ε_{xrmsn} and ε_{yrmsn} but also the higher beam intensity with the same maximum 2 MHz-RF power of 50 kW. The phenomena are understandable as the results of the enlarged effective extraction field and the more preferable focusing force in the extraction gap with the Φ_{EE} of 7.1 mm. This is consistent with the result of the unexpectedly degraded ε_{xrmsn} and ε_{yrmsn} for the smaller PE beam-hole-diameter (Φ_{PE}) reported in 2012.[9] The relationships between the I_{H^-} and the P_{RF} measured simultaneously with the measurements shown in Fig. 7 are shown in Fig. 8. The smaller Φ_{EE} than 7.1 mm is promising to improve the ε_{xrmsn}, ε_{yrmsn}, and I_{H^-} furthermore. The P_{RF} for Φ_{EE} of 8.3, 7.7, and 7.1 mm are plotted with open squares, triangles, and circles, respectively. Although the I_{H^-} for the Φ_{EE} of 8.3 mm is saturated at 69.3 mA with the PRF more than 46.6 kW, it for the Φ_{EE} of 7.1 mm is proportional to the P_{RF} up to 50 kW. The higher I_{H^-} should be produced with the P_{RF} higher than 50 kW for the Φ_{EE} of 7.1 mm. The measured horizontal emittances with the fitted normalized 1.5π mm mrad ellipses for the I_{H^-} of 33, 46, 60, 66, and 77 mA with the #4 PCH and the Φ_{EE} of 7.1 mm and G1.9 mm are plotted in Figs. 9(a1)–9(f1),

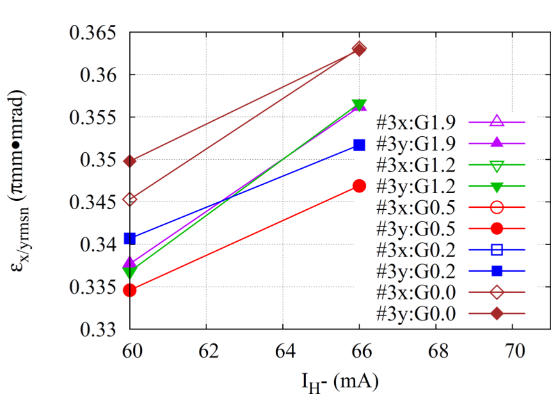

FIG. 4. Relationships between I_{H^-} and ε_{xrsmn} and ε_{yrsmn} measured for #3 PCH with RFMs gap lengths of G(0.0, 0.2, 0.5, 1.2, 1.9).

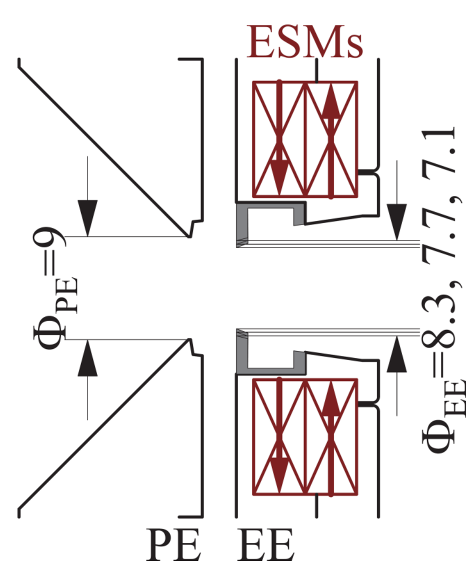

FIG. 6. Drawing of PE and EE magnified around beam-holes.

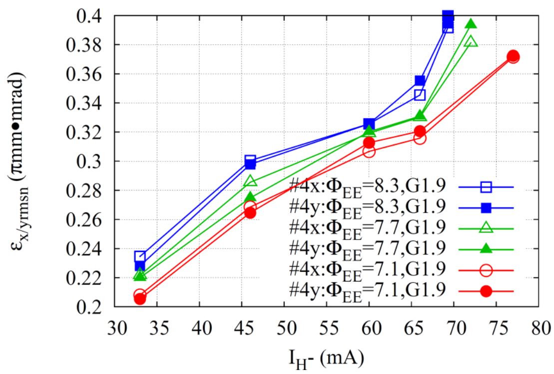

FIG. 7. Relationships between I_{H^-} and ε_{xrsmn} and ε_{yrsmn} measured for #4 PCH with Φ_{EE} of 8.3, 7.7, and 7.1 and RFM gap length G1.9 mm.

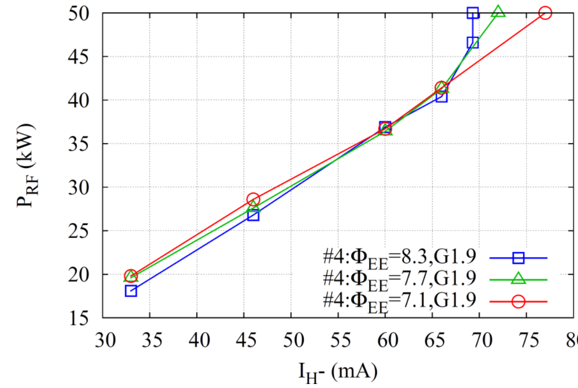

FIG. 8. Relationships between I_{H^-} and P_{RF} measured for #4 PCH with Φ_{EE} of 8.3, 7.7, and 7.1 mm and RFM gap length G1.9 mm.

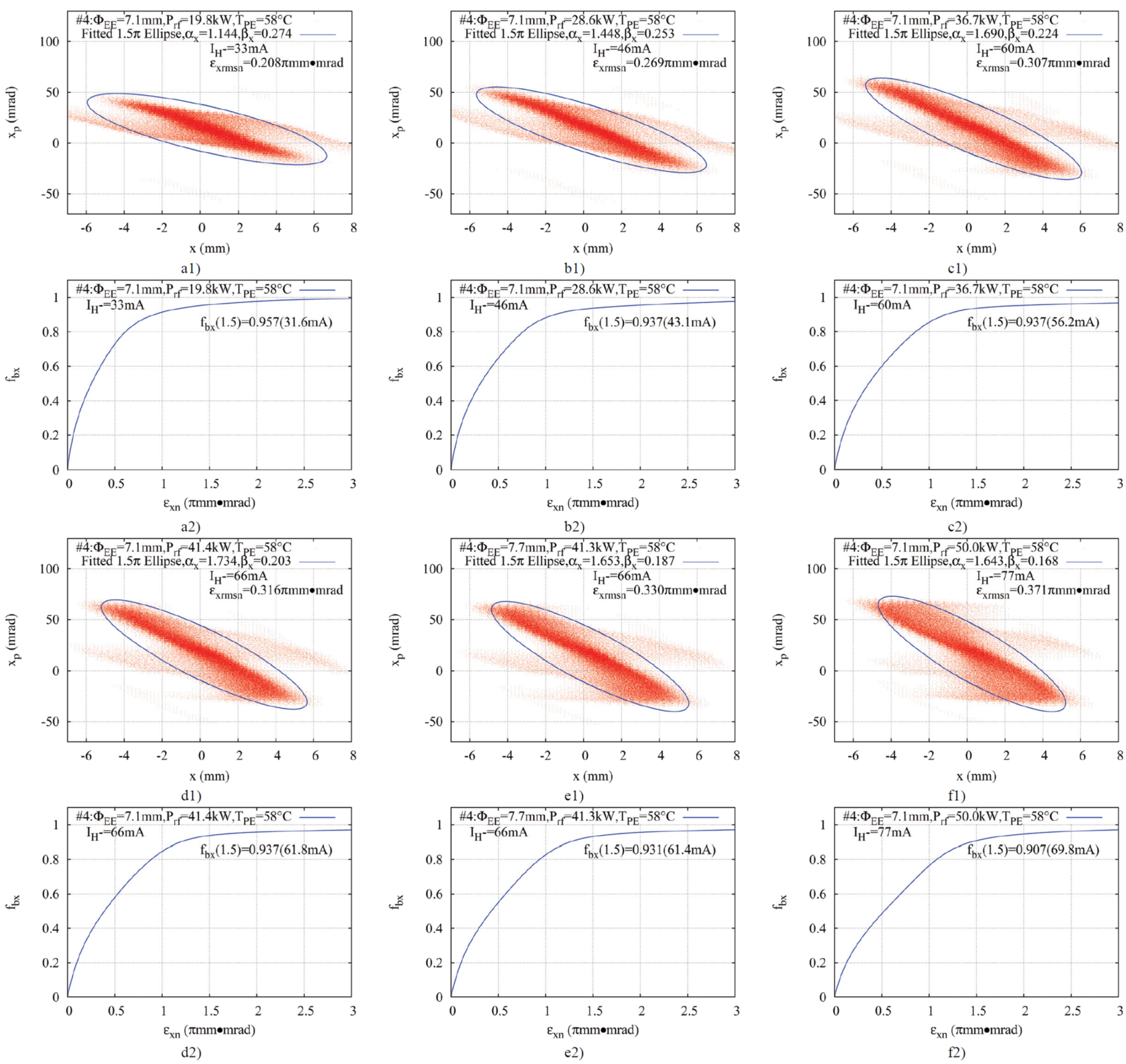

FIG. 9. Measured horizontal emittances with fitted normalized 1.5π mm mrad ellipses for I_{H^-} of 33, 46, 60, 66, and 77 mA with #4 PCH and Φ_{EE} of 7.1 mm and G1.9 mm are plotted in (a1), (b1), (c1), (d1), and (f1), respectively. Relationships between horizontal normalized emittances ε_{xn} with beam-fractions in them f_{bx} for I_{H^-} of 33, 46, 60, 66, and 77 mA with #4 PCH and the Φ_{EE} of 7.1 mm and G1.9 mm are plotted in (a2), (b2), (c2), (d2), and (f2), respectively. Measured horizontal emittance with fitted normalized 1.5π mm mrad ellipse for I_{H^-} of 66 mA with #4 PCH and Φ_{EE} of 7.7 mm and G1.9 mm is plotted in (e1). Relationship between horizontal normalized emittance ε_{xn} with beam-fraction in it f_{bx} for I_{H^-} of 66 mA with #4 PCH and Φ_{EE} of 7.7 mm and G1.9 mm is plotted in (e2).

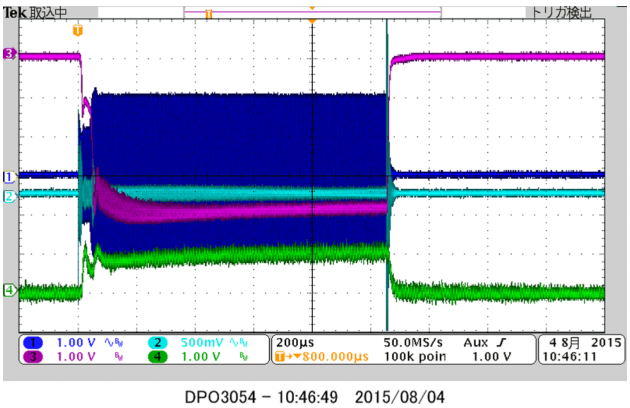

FIG. 10. Waveforms of 2 MHz-RF forward and reflected voltages (V_{RFF}: trace1 and V_{RFR}: trace2), H^- ion beam intensity (I_{H^-} 20 mA/Div.: trace3) and extraction current (I_{ext} 100 mA/Div.: trace4) measured with #2 PCH, Φ_{EE} of 7.1 mm, RFM gap length G1.9 mm, and RF-power of 50 kW. I_{H^-} averaged during initial 500 μs flat-top is 80 mA.

respectively. The relationships between the horizontal normalized emittances ε_{xn} with the beam-fractions in them f_{bx} for the I_{H^-} of 33, 46, 60, 66, and 77 mA with the #4 PCH and the Φ_{EE} of 7.1 mm and G1.9 mm are plotted in Figs. 9(a2)–9(f2), respectively. The measured horizontal emittance with the fitted normalized 1.5π mm mrad ellipse for the I_{H^-} of 66 mA with the #4 PCH and the Φ_{EE} of 7.7 mm and G1.9 mm is plotted in Fig. 9(e1). The relationship between the horizontal normalized emittance ε_{xn} with the beam-fraction in it f_{bx} for the I_{H^-} of 66 mA with the #4 PCH and the Φ_{EE} of 7.7 mm and G1.9 mm is plotted in Fig. 9(e2). The emittance (ε_{xrmsn} = 0.316π mm mrad) shown in Figs. 9(d1) and 9(d2) is improved from that (ε_{xrmsn} = 0.330π mm mrad) shown in Figs. 9(e1) and 9(e2) by decreasing the Φ_{EE} to 7.1 mm from 7.7 mm.

The waveforms of the forward and reflected 2 MHz-RF voltages (V_{RFF}: trace 1 and V_{RFR}: trace 2) measured with −60 dB directional couplers, the H^- ion beam intensity (I_{H^-} 20 mA/Div.: trace 3), and the extraction current (I_{ext} 100 mA/Div.: trace 4) were measured as in Fig. 10, in the operation with the Φ_{EE} of 7.1 mm, the #2 PCH and the maximum 2 MHz-RF power (P_{RF}) of 50 kW. The ε_{xrmsn} and ε_{yrmsn} with the #2 PCH and the Φ_{EE} of 7.7 mm were slightly smaller than those with other PCHs so far. The I_{H^-} averaged during the initial 500 μs flat-top is 80 mA, whose ε_{xrmsn} and ε_{yrmsn} were measured as 0.394 and 0.394 π mm mrad, respectively.

V. CONCLUSIONS

The triple-gap-lengths (Gs) of 0.5 mm for each of pairing five piece rod-filter-magnets were optimum to minimize the ε_{xrmsn} and ε_{yrmsn} with the #3 PCH. Since the ε_{xrmsn} and ε_{yrmsn} are still higher than those with other PCHs and the spike-noise-like fluctuations of the vacuum pressure, whose elements were identified as argon and nitrogen gases, were occasionally observed only with the #3 PCH, the larger degradation of the ε_{xrmsn} and ε_{yrmsn} was thought to be caused by the impurity gases. The grooves for the O-rings of the #3 PCH, which are suspected to produce the air-pockets, are under machining to remove them.

The smallest beam-hole-diameter of the extraction electrode (Φ_{EE}) of 7.1 mm among 8.3, 7.7, and 7.1 mm produced not only the smallest ε_{xrmsn} and ε_{yrmsn} but also the highest I_{H^-} with the maximum 2 MHz-RF power of 50 kW. The phenomena are understandable as the results of the enlarged effective extraction field and the more preferable focusing force in the extraction gap with the Φ_{EE} of 7.1 mm. The smaller Φ_{EE} than 7.1 mm will be used in near future in order to improve both of the ε_{xrmsn} and ε_{yrmsn} and the I_{H^-}.

ACKNOWLEDGMENTS

The authors wish to express their sincere thanks to Dr. Martin P. Stockli of the SNS and SNS ion-source group members for their support to purchase internal-RF-antennas and their information on the SNS RF-driven H^- ion-source.

[1]H. Oguri, K. Ohkoshi, K. Ikegami, A. Takagi, H. Asano, and A. Ueno, "Status of the RF-driven H^- ion source for J-PARC beam injector," Rev. Sci. Instrum. (these proceedings).
[2]A. Ueno, K. Ohkoshi, K. Ikegami, A. Takagi, S. Yamazaki, and H. Oguri, AIP Conf. Proc. **1655**, 030008 (2015).
[3]A. Ueno, K. Ohkoshi, K. Ikegami, A. Takagi, S. Yamazaki, and H. Oguri, AIP Conf. Proc. **1655**, 030009 (2015).
[4]A. Ueno, K. Ohkoshi, K. Ikegami, A. Takagi, S. Yamazaki, and H. Oguri, AIP Conf. Proc. **1655**, 030010 (2015).
[5]M. P. Stockli, B. Han, S. N. Murray, T. R. Pennisi, M. Santana, and R. F. Welton, Rev. Sci. Instrum. **81**, 02A729 (2010).
[6]A. Ueno, K. Ikegami, and Y. Kondo, Rev. Sci. Instrum. **75**(5), 1714 (2004).
[7]S. Yamazaki, A. Ueno, Y. Namekawa, K. Ohkoshi, I. Koizumi, K. Ikegami, A. Takagi, and H. Oguri, AIP Conf. Proc. **1515**, 433–439 (2013).
[8]See http://www.oceanoptics.co.jp/products/spectrometers/jaz-el200-xr.html for information on JAZ-EL200-XR.
[9]A. Ueno, Y. Namekawa, S. Yamazaki, K. Ohkoshi, I. Koizumi, K. Ikegami, A. Takagi, and H. Oguri, AIP Conf. Proc. **1515**, 417–424 (2013).